Molecular Neurobiology (2023) 60:4679–4692
https://doi.org/10.1007/s12035-023-03369-w

ORIGINAL ARTICLE

Microglia Signaling Pathway Reporters Unveiled Manganese Activation of the Interferon/STAT1 Pathway and Its Mitigation by Flavonoids

Valeri V. Mossine[1,2] · James K. Waters[2] · Grace Y. Sun[1] · Zezong Gu[3] · Thomas P. Mawhinney[1,2,4]

Received: 14 February 2023 / Accepted: 25 April 2023 / Published online: 4 May 2023

Abstract

Neuroinflammatory responses to neurotoxic manganese (Mn) in CNS have been associated with the Mn-induced Parkinson-like syndromes. However, the framework of molecular mechanisms contributing to manganism is still unclear. Using an in vitro neuroinflammation model based on the insulated signaling pathway reporter transposon constructs stably transfected into a murine BV-2 microglia line, we tested effects of manganese (II) together with a set of 12 metal salts on the transcriptional activities of the NF-κB, activator protein-1 (AP-1), signal transducer and activator of transcription 1 (STAT1), STAT1/STAT2, STAT3, Nrf2, and metal-responsive transcription factor-1 (MTF-1) via luciferase assay, while concatenated destabilized green fluorescent protein expression provided for simultaneous evaluation of cellular viability. This experiment revealed specific and strong responses to manganese (II) in reporters of the type I and type II interferon-induced signaling pathways, while weaker activation of the NF-κB in the microglia was detected upon treatment of cells with Mn(II) and Ba(II). There was a similarity between Mn(II) and interferon-γ in the temporal STAT1 activation profile and in their antagonism to bacterial LPS. Sixty-four natural and synthetic flavonoids differentially affected both cytotoxicity and the pro-inflammatory activity of Mn (II) in the microglia. Whereas flavan-3-ols, flavanones, flavones, and flavonols were cytoprotective, isoflavones enhanced the cytotoxicity of Mn(II). Furthermore, about half of the tested flavonoids at 10–50 μM could attenuate both basal and 100–200 μM Mn(II)-induced activity at the gamma-interferon activated DNA sequence (GAS) in the cells, suggesting no critical roles for the metal chelation or antioxidant activity in the protective potential of flavonoids against manganese in microglia. In summary, results of the study identified Mn as a specific elicitor of the interferon-dependent pathways that can be mitigated by dietary polyphenols.

Keywords Manganese · *piggyBac* transposon · Interferon-sensitive response element ISRE · Apigenin · Myricetin · EGCG

Introduction

Numerous observational and experimental studies have established an association between environmental pollutants and elevated risk of various neurological disorders in humans. To this end, overexposure to or dysregulation of metals in CNS has been implicated in Alzheimer's, Parkinson's, and Wilson's diseases [1, 2]. One of such metals is manganese, an important bioelement, which is also extensively used by humans, especially as a component of stainless-steel alloys. The Parkinson disease-like symptoms, which appear as a result of excessive manganese accumulation in the brain and which could not be ameliorated by dopamine precursor levodopa [3], had been recorded for many years in workers exposed to Mn-containing aerosols at steel mills, mines, or welding [4] and are currently known

✉ Valeri V. Mossine
mossinev@missouri.edu

1 Department of Biochemistry, University of Missouri, Columbia, MO 65211, USA

2 Agriculture Experiment Station Chemical Laboratories, University of Missouri, Columbia, MO 65211, USA

3 Department of Pathology and Anatomical Sciences, University of Missouri, Columbia, MO 65211, USA

4 Department of Child Health, University of Missouri, Columbia, MO 65211, USA

as manganism symptoms. However, molecular and cellular mechanisms of the manganese neurotoxicity are not yet fully understood. A limited number of agents have been proposed to attenuate neurotoxicity of manganese, including polyphenols silymarin [5], resveratrol [6], curcumin [7], and quercetin [8], metal chelators EDTA [9], *p*-aminosalicylic acid [10, 11], and antioxidant RibCys [12]. Nonetheless, no effective therapy currently exists to treat manganese poisoning in the brain.

Microglia are macrophage-like cells residing in the CNS. These cells are charged with a variety of brain defense and homeostasis tasks, from scavenging infected and damaged cells or cell debris to regulating regeneration and remodeling of the brain neuronal networks [13]. Transformation of microglia to reactive states in response to pathological stimuli, or microglial activation, can also be neurotoxic and contribute to the neurodegenerative processes in the brain [14]. Thus, it has been proposed that cellular mechanisms of Mn neurotoxicity may involve, among others, disruption of function and chronic inflammatory activation of microglia and astrocytes [15]. Suggested molecular mechanisms of Mn cytotoxicity implicate oxidative stress, impairment of glutaminase activity, and transcriptional and functional deregulation of the glutamate transporters in glial cells [16, 17]. The suggested pathways involved in Mn-induced inflammatory activation of glial cells have been limited, so far, to the signaling cascades of NF-κB [15, 18] and JAK2/STAT3 [19] pathways plus subsequent production of pro-inflammatory inducible nitric oxide synthase (iNOS), cyclooxygenase-2 (COX-2), interferon-alpha, interferon-beta, and interferon-gamma (IFN-α/β/γ), tumor necrosis factor (TNFα), interleukin-1β and interleukin-6 (IL-1β, IL-6) [20, 21]. In addition, Sengupta et al. [22] reported a gene expression profile in manganese chloride-treated primary human astrocytes and, according to this report, out of 20 targets positively affected by the IFN-γ/JAK/STAT1 pathway, sixteen were upregulated by Mn. Based on these findings, it could be hypothesized that pro-inflammatory signaling stimulated by Mn in microglia may include the IFN-γ pathway, as well.

Signal transducer and activator of transcription 1 (STAT1) is a cytoplasmic inducible transcription factor which relays extracellular signals, typically provided by type I (IFN-α, β, δ, etc.), type II (IFN-γ), or type III (IFN-λ) interferons and certain cytokines [23, 24]. Two principal signaling pathways leading to activation of STAT1 involve recognition of the interferons by, respectively, type I/type III or type II interferon receptors, a subsequent activation of associated Janus tyrosine kinases (JAKs), and phosphorylation of cytoplasmic STAT1 by JAK. Activated STAT1 then forms either homodimer or heterodimer with STAT2. The homodimer STAT1 is directly translocated to the nucleus, where it regulates gene expression at the gamma-interferon activated DNA site (GAS). The heterodimer STAT1/2 forms a complex with Interferon Regulatory Factor 9 (IRF9) and then binds to DNA, predominantly at a different gene regulatory sequence called interferon-stimulated response element (ISRE). When bound to the GAS, the STAT1 can upregulate production of a number of pro-inflammatory enzymes and mediators, including NOS2, COX-2, TNF-α, IL-1β, IL-6, IL-12, IL-23, MCP-1, or IFN-γ [25, 26]. As a consequence, IFN activation of STAT1 in microglia and peripheral macrophages may promote their transformation into the pro-inflammatory phenotypes [27, 28].

Recently, we have reported a successful application of insulated reporter transposons in astrocytes for assessment of activity of multiple neuroinflammation-related transcription factors, including the STAT1 [29]. In this paper, we describe testing of the reporter construct in BV-2 microglia cell line, by taking on an objective of searching for potential pro-inflammatory metals and their inhibitors in microglia. Here, we report for the first time activation of the gamma-interferon-dependent JAK/STAT1 pathway in Mn-treated microglial cells. Next, we describe the effects of 64 flavonoids on the transcription factors implicated in neuroinflammation, namely STAT1, STAT1/2, STAT3, NF-κB, AP-1, and Nrf2. Finally, we elucidate the preventive potential of the flavonoids against manganese-induced transcriptional activation of the homodimer STAT1.

Materials and Methods

Chemicals

A collection of metal salts, biochemicals, and flavonoids was from various reagent vendors (Supplementary Table S1). The compounds were of reagent grade (> 90%) and used without further purification. Stock solutions of flavonoids were prepared in DMSO/propylene glycol (1:3 v/v) at 20 mM concentrations and were stored at − 20 °C until use. Lipopolysaccharide (LPS) from *Pseudomonas aeruginosa* was purchased from MilliporeSigma.

Cell Culture

Immortalized murine microglia cell line BV-2 [30] was provided by Dr. Grace Sun (University of Missouri) who received an original batch from Dr. Rosario Donato (University of Perugia, Italy). The cells, as well as the BV2-based reporter transfects, have been routinely cultured in 1:1 DMEM/F12 Ham media mixture (MilliporeSigma) supplemented with 5% newborn calf serum (NCS, HyClone) and 1% (v/v) penicillin/streptomycin cocktail (pen/strep, HyClone). This medium is henceforth referred to as the DMEM/F12 complete medium. To passage, the cells were treated with 0.05% trypsin (MP Biochemicals) in 1:1

Corning CellStripper cocktail/PBS (MilliporeSigma) and subcultured at 1:5 ratio upon reaching 60–70% confluency. The standard culturing conditions for all cells were 37 °C, 5% CO_2, and 100% humidity.

Plasmid Constructs

Super *piggyBac* transposase expression vector was purchased from System Biosciences. Vectors *p*TR01F, *p*TR05F, *p*TR09F, *p*TR13F, *p*TR23F, and *p*TR34F have been previously reported [29, 31, 32]. *p*TR25F vector has been assembled as follows: inserts containing 4-bp overhang sequences for the ligation reaction and total of 8 interferon-sensitive response elements (ISRE) for binding the heterodimer transcription factor STAT1/STAT2 (Table 1) were synthesized and annealed. The inserts and the larger product of *p*TR01F [31] digestion with the *Nhe*I/*Bgl*II were uniformly assembled into *p*TR25F in one ligation step. Correctness of the insertion was confirmed by DNA sequencing.

Stable Transfections

To generate stable reporter BV2.RnnF lines, the original BV-2 cells were seeded into wells of a 96-well plate, at 5 × 10^4 cells per well in complete DMEM/F12 medium and left to adhere for 6 h. The cells were then treated with the NATE inhibitor cocktail (InvivoGen) for 30 min, followed by a mixture of 100 ng *p*TRnnF reporter plasmids and 33 ng Super *piggyBac* transposase plasmid complexed with Lipofectamine 2000 transfection reagent (Invitrogen) at 1:2 (µg DNA/ µL reagent) ratios. After 16 h, regular media were added and cells were left to proliferate for the next 48–72 h. The transfected cells were then treated with the selecting antibiotic (5 µg/mL puromycin) for another week, and the surviving cells were expanded for cryopreservation and activity validation. When the numbers of reporter cells were expanded for experiments, the complete DMEM/F12 medium was typically supplemented with 2 µg/mL puromycin.

Table 1 Octamer interferon-sensitive response element sequences for the construction of *p*TR25F vector

Insert	Sequence
Sense	ctagcTAGTTTCACTTTCCCTAGTTTCAC TTTCCCTAGTTTCACTTTCCCTAGTTT CACTTTCCCTAGTTTCACTTTCCCTAG TTTCACTTTCCCTAGTTTCACTTTCCC TAGTTTCACTTTCCCa
Antisense	gatctGGGAAAGTGAAACTAGGGAAAGTG AAACTAGGGAAAGTGAAACTAGGG AAAGTGAAACTAGGGAAAGTGAAACTA GGGAAAGTGAAACTAGGGAAAGTG AAACTAGGGAAAGTGAAACTAg

Cell Treatment Schedule

Typically, original BV-2 or reporter BV2.RnnF cells were plated in Nunclon Delta Edge 96-well plates (ThermoFisher) at 1 × 10^4 cells/well in 100 µL of an adaptation low-serum medium consisted of the DMEM/F12 media mixture supplemented with 2 mg/L insulin, 2 mg/L transferrin, 2 µg/L selenite (2-ITS), 2% NCS, and the pen/strep antibiotic. After 40 h, the adaptation medium was replaced with the Phenol Red-free 5:5:1 DMEM/F12/RPMI-1640 mixture, supplemented with 1 g/L BSA, the 2-ITS mix and the pen/strep (the test medium). The cells were cultured for next 6 h, after which time, the medium was replaced with fresh test medium containing 0.5% of the DMSO/propylene glycol mix (carrier solvent controls), metal salts, flavonoids, and/or specific inducer agents, and the plates were incubated for the next 18 h or other indicated times.

Reporter Activity Assay

In a typical experiment, immediately after the treatments, the reporter cells in 96-well plates were carefully washed with PBS and lysed in 70 µL of the lysing buffer [29] for 16 h at 8 °C. The GFP fluorescence values in the lysates were measured at the 482(9)/512(17) nm wavelength (slit width) setup and was followed by an addition of 20 µL luciferase substrate [29]. Kinetic luminescence readings in the wells were done in 2-min intervals for 8 min total. All the measurements were done using a Synergy MX (BioTek) plate reader. The GFP fluorescence values were used for both evaluation of relative cell transcriptional activity/proliferation and normalization of the reporter luciferase activities in respective wells.

Plotting and Statistical Analysis

Statistical tests and plots were done using SigmaPlot, version 13.0. Datasets are presented as mean ± SD. Individual data points are plotted where applicable.

Results

Validation of BV-2 Reporters

A general scheme of the reporter constructs used in this study is shown in Fig. 1A. We have developed a unique set of insulated, *piggyBac* transposable reporters consisting of a specific transcription factor response element to regulate expression of the firefly luciferase gene. The elongation factor 1 (EF1) promoter for continuous activation of the copepod GFP gene fused with a puromycin resistance sequence allows for simultaneous evaluation of cellular viability,

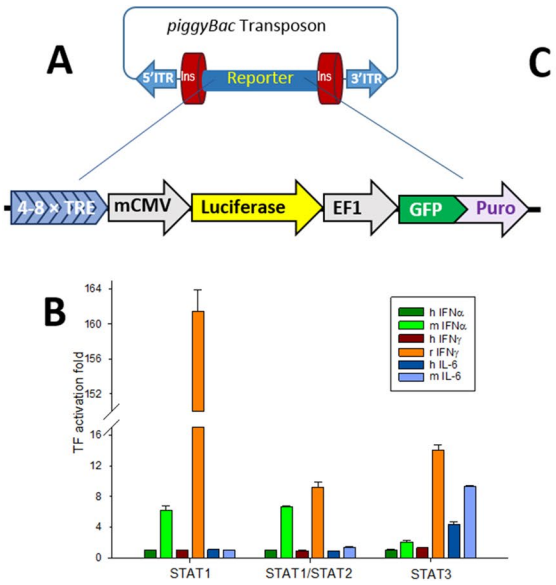

C

NF-κB	AP-1	STAT1	STAT1/2	STAT3	Nrf2	MTF-1	
2.867	-0.148	1.166	0.873	-1.045	0.698	-1.129	TNFα
4.901	-0.654	1.041	1.514	-1.458	2.482	-2.560	LPS
2.138	-0.252	-0.272	1.311	-0.422	0.336	-0.840	poly(I:C)
0.340	0.966	-0.432	0.354	-0.737	1.929	-0.319	PMA
-4.042	-2.117	-2.850	1.125	-0.429	4.767	-1.629	CDDO-Me
-1.022	-0.141	-1.097	2.464	0.104	4.693	-0.253	tBHQ
-0.289	-0.838	-0.568	0.968	-0.164	2.176	-1.871	H_2O_2
0.055	-0.042	0.058	1.528	1.455	4.977	-0.009	pyocyanin
-0.727	-1.944	-1.614	-1.587	0.725	3.319	-1.554	o-phen
0.111	-0.014	-0.308	-0.062	-0.185	1.979	2.420	$ZnCl_2$
-0.314	0.010	2.647	2.734	1.074	-0.372	0.046	IFNα
0.428	-1.106	7.595	3.406	3.809	-2.626	-3.423	IFNγ
-0.017	-0.198	0.122	-0.132	3.217	-0.352	0.016	IL-6
-0.628	0.032	-1.007	-0.434	0.333	-0.271	0.076	IL-4
-1.198	-0.376	0.090	0.044	-0.711	-1.101	-0.787	Dasatinib
-0.554	-0.020	-3.372	-0.061	-1.218	-0.290	-0.017	Ruxolitinib
-4.262	-0.798	-4.081	0.749	-1.174	4.079	-0.253	AG490

Fig. 1 Establishing transcriptional activation assay in immortalized murine microglia BV-2. **A** A general scheme of the reporter construct. Four to eight specific transcription factor binding sequences (transcription factor response elements, TREs) and the mCMV promoter regulate reporter firefly luciferase, while the EF1 promoter provides constant production of destabilized copepod GFP and puromycin resistance selector. The flanking insulators protect from epigenetic silencing of the reporter, while the *piggyBac* transposon ITRs secure accurate and efficient insertion of the reporter into the genomic DNA. **B** Comparative TF activity in reporter cells treated with human vs rodent pro-inflammatory cytokines. Concentrations of human and murine cytokines, 20 ng/mL; rat interferon-γ, 2 ng/mL. The error bars are SDs for $n = 3$. **C**. Heatmap of the reporter activation, expressed as $\log_2$(TF induction fold), to common inducers and inhibitors used to validate specificity of the reporters. See extended Supplementary Table S2 for viabilities and SDs. Concentrations: tumor necrosis factor (TNFα), 5 ng/mL; lipopolysaccharide (LPS), 100 ng/mL; poly(I:C), 5 μg/mL; phorbol 12-myristate 13-acetate (PMA), 100 ng/mL; Bardoxolone (CDDO-Me), 500 nM; *tert*-butyl hydroquinone (tBHQ), 10 μM; hydrogen peroxide, 250 μM; pyocyanin, 60 μM; *o*-phenanthroline, 20 μM; $ZnCl_2$, 20 μM; mouse interferon-α (m IFNα), 10 ng/mL; rat interferon-γ (r IFNγ), 5 ng/mL; mouse interleukin-6 (m IL-6), 10 ng/mL; mouse interleukin-4 (IL-4), 25 ng/mL; Dasatinib, 200 nM; Ruxolitinib, 50 nM; Tyrphostin B42 (AG490), 50 μM

normalization of the luciferase activity, and selection of cells with the reporter resistant to epigenetic silencing. In addition to previously reported plasmids [29, 31, 32], we have assembled a novel reporter vector that carries eight binding sites, ISRE sequences, for the heterodimer transcription factor STAT1/STAT2. The BV-2 microglia were stably transfected with this plasmid, as well as with the reporters for transcriptional activity of the NF-κB, AP-1, homodimer STAT1, STAT3, Nrf2, and MTF-1. The new reporter cell lines were tested for selectivity (Fig. 1, Supplementary Table S2). As expected, activity of the NF-κB, AP-1, STAT1, STAT1/STAT2, STAT3, and MTF-1 increased upon treatment of the microglia with respective specific inducers, namely LPS, PMA, IFN-γ, IFNα, IL-6, CDDO-Me, and $ZnCl_2$. Microglia were particularly sensitive to IFN-γ, which induced over hundredfold increase in the STAT1 activity. Interestingly, transcriptional activity of the STAT1/STAT2, but not the NF-κB, AP-1 and STAT1, significantly increased upon treatment of the microglia with redox stressors and classical inducers of Nrf2 such as bardoxolone, *tert*-butyl hydroquinoline, hydrogen peroxide, and pyocyanin [32]. Among other surprising responses were high inhibitory activity of IFN-γ against MTF-1 and the anti-inflammatory effects of an iron chelator *o*-phenanthroline. Murine BV-2 microglia did not recognize human IFN-α and IFN-γ but was species-tolerant towards IL-6 (Fig. 1B).

Manganese Uniquely Induces Transcriptional Activities of the NF-κB, STAT1, and STAT1/2

To explore the pro-inflammatory responses in the newly developed set of BV-2 microglia-based reporters, we exposed the cultured microglia to 13 metal salts, which are of common interest to the neurotoxicology field. This initial testing revealed surprisingly strong responses in manganese-treated reporters for transcriptional activity of the homodimer STAT1 and heterodimer STAT1/STAT2 (Table 2). In addition to these interferon-dependent signaling pathways, manganese also induced activation of the pro-inflammatory NF-κB and JAK/STAT3 pathways, although to a much smaller effect. Among the rest of tested metal salts, only 1 mM barium chloride promoted activation of the NF-κB to a comparable extent. Barium did also promote activation of the oxidative/electrophilic stress sensor KEAP-1/Nrf2, as

Table 2 Activation folds of seven transcription factors in BV-2 microglia exposed to metal salts for 14 hours. See Supplementary Figures S1 –S7 for extended viability and dose-response data

metal	conc	NF-kB	AP-1	STAT1	STAT1/2	STAT3	Nrf2	MTF-1
Al(III)	1 mM	0.30	1.13	0.72	0.73	1.11	0.76	0.83
Ba(II)	1 mM	2.68	0.60	0.47	1.29	0.45	6.20	1.11
Cd(II)	10 µM	0.37	0.27	0.25	0.81	1.37	18.65	4.50
Co(II)	250 µM	0.85	1.40	0.40	1.32	0.54	20.55	2.72
Cr(III)	1 mM	0.58	1.02	1.04	0.57	0.20	1.33	0.91
Cr(IV)	25 µM	0.72	0.52	0.26	0.46	0.38	1.54	0.36
Cu(II)	20 µM	0.52	1.12	0.88	0.96	1.30	1.01	0.93
Fe(III)	1 mM	0.59	0.78	0.53	1.22	0.68	3.26	0.83
Mn(II)	125 µM	3.43	0.15	18.87	19.87	2.21	0.82	0.03
Ni(II)	250 µM	0.32	0.51	0.27	0.62	0.33	1.60	0.85
Pb(II)	50 µM	0.28	0.50	0.13	0.59	0.76	5.09	0.16
V(V)	125 µM	0.41	0.31	0.19	0.04	0.43	13.03	0.09
Zn(II)	40 µM	1.17	0.81	0.81	0.96	0.88	13.29	5.88

did other established Nrf2 activators Cd(II), Co(II), Fe(III), Pb(II), V(V), and Zn(II), at tested metal concentrations. Notably, manganese (II) had no effect on the transcription factor Nrf2 but exerted a strong inhibition of the MAPK/JNK/AP-1 and zinc-sensory MTF-1 pathways.

Next, we have assessed a comparative temporal activation of the interferon-dependent and the NF-κB signaling pathways in BV-2 microglia by manganese (II) and interferon-γ. As illustrated in Fig. 2, both IFNγ- and Mn(II)-induced activation of the pathways proceeded through maxima, which, in the IFNγ-treated reporter cells, were achieved in about 10 h. The activation of microglia treated with Mn(II) lagged until about 6 h, then reached maxima at about 12 and 15 h in the reporters of the interferon-dependent and the NF-κB signaling pathways, respectively.

We further asked whether Mn(II) could interact with specific pro-inflammatory activators at the ISRE and GAS in microglia. A number of previous studies have demonstrated the ability of Mn to potentiate effects of the NF-κB activators, such as LPS, TNFα, or IFNγ [20, 33]. Accordingly, we tested combinations of manganese (II) with IFNα, IFNγ, LPS, poly(I:C), and β-amyloid peptide (25-35) in the reporters of STAT1 and STAT1/2 transcriptional activation in microglia. There were no or weak interactions between Mn(II) and the interferons, poly(I:C), and $A\beta_{25\text{-}35}$ (Supplementary Tables S3–S7). However, the Mn(II)/LPS combinations revealed a trend of the antagonism at increasing concentrations of these agents (Table 3). The same trend was observed for the IFNγ/LPS combinations (Table 3).

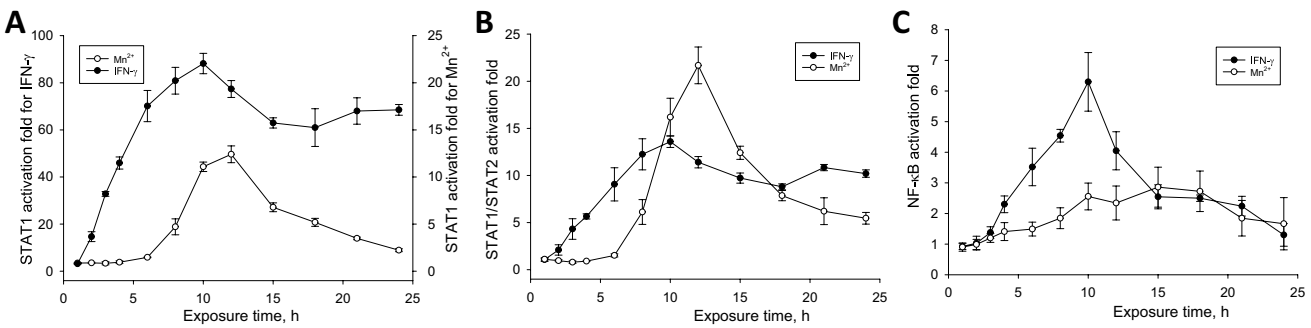

Fig. 2 Time course of transcriptional activation of the **A** homodimer STAT1, **B** heterodimer STAT1/STAT2, and **C** NF-κB transcription factors in BV-2 microglia exposed to 2 ng/mL IFN-γ or 100 µM manganese(II) citrate. The experimental curves in **A** have been drawn to different scales, for clarity

Table 3 Relative TF activation folds in BV-2 microglia treated with combinations of LPS and Mn(II) or combinations of LPS and IFNγ for 12 h, the data points are single measurements. In each row, the activation folds are normalized to Mn(II)-only treated cells at indicated Mn(II) concentrations (Supplementary Table S3). Data highlighted in blue indicate antagonistic interactions between Mn(II) and LPS or between IFN-γ and LPS in microglia

Transcription Factor →	STAT1						STAT1/STAT2					
LPS, ng/mL	0	2	8	32	128	512	0	2	8	32	128	512
Mn^{2+}, μM												
0	1.00	1.24	1.52	2.21	2.69	3.11	1.00	1.71	2.27	3.83	4.56	5.10
21	1.00	0.97	1.15	1.67	2.11	2.78	1.00	0.86	1.81	2.34	2.93	3.65
30	1.00	1.21	1.38	1.85	2.26	2.74	1.00	1.16	1.72	2.54	3.21	3.43
42	1.00	1.08	1.14	1.34	1.89	2.09	1.00	1.09	1.33	1.82	2.06	2.22
58	1.00	1.13	1.27	1.37	2.21	2.50	1.00	1.18	1.43	2.04	1.97	2.15
82	1.00	0.77	1.06	0.72	0.71	0.71	1.00	1.90	1.80	2.18	1.55	1.46
114	1.00	1.02	0.83	0.50	0.47	0.47	1.00	1.35	1.46	1.08	0.77	0.52
160	1.00	0.96	0.76	0.58	0.46	0.41	1.00	1.14	0.89	0.73	0.47	0.40
IFNγ, ng/mL												
0	1.00	1.24	1.95	2.78	3.17	3.25	1.00	1.20	1.27	1.76	2.22	2.45
0.063	1.00	1.23	1.27	1.16	1.15	0.95	1.00	1.22	1.32	1.45	1.48	1.45
0.125	1.00	1.00	0.99	0.76	0.65	0.51	1.00	1.00	1.00	1.05	1.09	0.95
0.25	1.00	0.82	0.64	0.53	0.47	0.38	1.00	1.12	1.06	0.89	0.90	0.77
0.5	1.00	0.72	0.71	0.55	0.39	0.38	1.00	0.89	0.93	0.81	0.75	0.60
1	1.00	0.73	0.68	0.58	0.47	0.38	1.00	0.96	0.93	0.79	0.78	0.60
2	1.00	0.76	0.69	0.59	0.51	0.43	1.00	0.93	0.87	0.80	0.68	0.60
4	1.00	0.75	0.73	0.54	0.52	0.50	1.00	0.98	0.92	0.78	0.70	0.59

Flavonoids Differentially Affect Basal Activities of the Neuroinflammation-Related Transcription Factors NF-κB, AP-1, STAT1, STAT1/STAT2, STAT3, and Nrf2

In order to demonstrate the utility of our microglia-based reporters for high-throughput protocols, we performed evaluation of multiple natural and synthetic flavonoids as potential inducers/inhibitors of signaling pathways implicated in neuroinflammation. Specifically, in a single experiment, we tested 64 flavonoids (Supplementary Table S1), at two concentrations, 10 μM and 50 μM, 3 samples per agent dose, in 6 reporter lines. Together with the assay controls, about 2500 biological samples were processed in one run, yielding about 5000 data points, given that each biological sample provided a cell lysate for the GFP fluorescence and luciferase luminescence readouts. The results of the experiment are summarized in Fig. 3 and Supplementary Table S8. There is a significant variability in the reporter responses to individual flavonoids, but certain patterns can be seen in Fig. 3. Thus, structural classes of flavan-3-ols and anthocyan(id)ins generally suppress the basal levels of all six transcriptional factors, while flavones and isoflavones induce an increase in activities of these TFs. Several individual flavonoids, including flavone, chrysin, acacetin, daidzein, formononetin, genistein, and biochanin A, acted as "pan-activators" of all six signaling pathways in the reporter microglia. Among the reporters, STAT1 was the most sensitive to inhibition by flavonoids, while the redox sensor Nrf2 was activated by the majority of tested flavonoids at 50 μM.

Effects of Flavonoids on Manganese Cytotoxicity and Manganese-Induced Transcriptional Activation of the Homodimer STAT1

Having found that certain flavonoids can significantly inhibit basal activity of the type II interferon signaling pathway in BV-2 microglia, we also examined whether flavonoids could inhibit the manganese-promoted activation of this pathway. Cells were treated with combinations of 100 μM or 200 μM manganese(II) and 50 μM flavonoid for 12 hours. The chosen Mn(II) concentrations were close to pathophysiological levels of manganese (60–160 μM) found in the human brain [34]. In addition, this experiment included treating microglia with combinations of the 50 μM flavonoids with interferon-γ at 1 ng/mL. The results are given in Supplementary Table S9 and are illustrated in Fig. 4. Analysis of Fig. 4 reveals an overall trend of flavonoids to

			NF-κB		AP-1		STAT1		STAT1/2		STAT3		Nrf2	
			10 μM	50 μM	10 μM	50 μM	10 μM	50 μM	10 μM	50 μM	10 μM	50 μM	10 μM	50 μM
flavanols	1	catechin	0.947	0.562	-0.151	-0.162	0.219	0.352	0.201	-0.072	-0.074	0.262	-0.483	-0.611
	2	epicatechin	0.648	0.280	-0.201	-0.209	0.062	0.143	-0.209	-0.059	0.141	0.477	-0.582	-0.616
	3	ECG	0.526	0.469	-0.211	-0.372	-0.084	-0.026	-0.237	0.234	0.115	0.006	-0.075	0.455
	4	GC	0.319	0.058	-0.090	-0.180	0.119	-0.138	-0.155	-0.290	0.158	0.168	-0.257	0.379
	5	EGC	-0.037	0.284	-0.085	-0.233	0.102	-0.077	-0.154	-0.402	0.183	0.292	-0.578	-0.680
	6	EGCG	0.158	-0.085	-0.131	-0.324	0.057	0.143	-0.127	-0.210	0.017	0.000	-0.157	0.390
flavanones	7	naringenin	0.385	0.602	0.165	0.785	0.248	0.778	0.077	0.774	0.076	1.268	0.195	1.137
	8	naringin	0.473	0.399	0.107	-0.066	-0.161	-0.198	-0.436	0.145	-0.117	-0.021	0.124	-0.076
	9	eriodictyol	0.095	0.746	-0.008	0.340	-0.910	-1.793	-0.561	0.262	0.404	-0.111	-0.306	1.097
	10	hesperetin	0.065	1.667	0.116	1.451	-0.068	0.856	-0.046	1.313	0.617	1.690	0.580	1.741
	11	hesperidin	0.222	0.293	0.041	0.148	-0.478	0.434	-0.329	0.201	0.153	0.229	-0.269	0.035
	12	taxifolin	0.323	0.040	0.008	0.168	0.027	0.077	-0.375	0.188	0.282	0.484	-0.531	-0.434
	13	silybin=silibinin	-0.084	-0.204	0.040	0.220	0.172	-0.242	-0.202	-0.083	0.183	-0.085	-0.056	0.383
flavones	14	flavone	2.043	2.607	1.276	1.043	1.462	0.544	1.284	0.827	1.675	1.950	1.584	2.517
	15	α-naphthoflavone	2.427	1.819	0.818	-1.065	0.890	-2.254	0.267	-0.589	0.497	-1.752	1.145	2.533
	16	7-OMe-flavone	1.710	2.820	1.315	1.103	1.754	1.356	1.364	1.232	1.221	1.442	1.324	2.277
	17	3',4'-(OH)2-flavone	0.179	0.093	0.497	-0.295	-1.423	-1.643	0.113	-0.645	0.281	-0.915	0.525	2.469
	18	4',5'-(OH)2-flavone	1.019	1.415	1.125	0.516	0.462	-0.904	0.649	0.178	1.098	-0.041	1.917	2.933
	19	4',7-(OMe)2-flavone	1.273	2.725	1.334	1.131	0.906	0.031	1.201	0.488	1.278	0.418	1.595	2.465
	20	5,6-(OH)2-flavone	0.667	0.458	0.982	0.296	0.233	-2.607	0.718	-0.184	1.053	-0.936	0.943	3.614
	21	chrysin	0.922	1.663	1.274	1.337	1.340	1.018	1.592	1.582	1.439	1.248	1.500	1.867
	22	7,8-(OH)2-flavone	0.092	0.174	0.280	0.607	-0.118	-1.138	0.038	0.644	0.455	0.602	-0.229	1.563
	23	2',3',6-(OH)3-flavone	0.727	0.533	0.037	0.969	0.042	-0.233	0.199	0.667	0.047	0.872	-0.464	1.913
	24	3',7,8-(OH)3-flavone	-0.156	-0.010	-0.007	0.017	-0.217	-1.448	-0.205	-0.399	0.142	-0.021	-0.569	0.294
	25	apigenin	0.985	2.188	1.273	1.067	0.391	-0.471	1.349	0.835	1.031	0.072	2.080	2.004
	26	acacetin	1.319	2.248	1.692	1.782	1.114	0.258	1.441	1.600	1.499	0.980	1.940	2.462
	27	4',7,8-(OH)3-flavone	-0.308	-0.182	-0.020	0.024	-0.082	-0.052	-0.214	-0.030	0.211	0.298	-0.544	0.161
	28	baicalein	-0.379	0.196	0.396	0.839	0.132	-0.303	0.388	0.419	0.357	0.678	-0.534	1.213
	29	baicalin	0.001	0.514	0.583	1.126	0.150	0.354	-0.062	0.828	0.102	0.605	-0.509	0.728
	30	wogonin	-0.295	0.681	-0.147	0.556	-0.562	-0.191	-0.289	0.693	0.015	0.713	0.081	1.219
	31	luteolin	0.196	1.050	0.234	0.797	-0.379	-1.607	-0.880	0.066	-0.406	-0.976	0.156	2.128
	32	diosmin	-0.052	-0.774	-0.088	-0.133	0.085	-0.251	-1.340	0.123	-0.070	-0.277	-0.134	0.188
	33	neodiosmin	0.100	-0.291	0.003	0.008	0.327	0.304	-0.581	-0.120	-0.097	0.319	-0.236	-0.297
	34	vitexin	-0.171	0.282	-0.073	-0.017	0.515	0.336	-0.471	-0.230	0.077	0.330	-0.276	-0.301
	35	tangeretin	-0.512	0.807	0.280	0.526	0.678	-0.155	0.139	-0.084	0.330	0.666	0.519	1.468
flavonols	36	flavonol	-0.333	1.413	-0.002	0.921	0.173	-2.716	-0.379	0.626	0.376	0.359	0.345	3.374
	37	4'-OMe-flavonol	0.386	-0.019	0.027	0.247	0.265	1.003	-0.592	0.206	0.032	0.373	0.377	0.862
	38	galangin	-0.015	1.067	-0.194	1.247	0.216	0.474	-0.275	0.784	0.039	1.275	0.913	2.884
	39	fisetin	-0.253	0.129	0.083	0.617	-0.325	-1.863	-0.333	0.799	0.304	-0.060	-0.002	1.355
	40	kaempferol	0.011	1.197	0.043	1.108	-0.403	0.618	-0.333	0.917	0.194	1.622	0.843	3.289
	41	4',7,8-(OH)3-flavonol	-0.287	-0.640	-0.063	-0.174	0.290	-2.177	-0.697	0.934	0.252	-0.433	-0.335	0.420
	42	morin	-0.468	-0.165	-0.009	0.231	0.039	0.407	-0.767	-0.215	0.280	0.513	-0.280	0.135
	43	quercetin	-0.646	-0.429	0.023	0.287	0.380	-0.944	-0.139	0.092	0.603	0.557	-0.265	0.252
	44	rhamnetin	-1.161	-1.649	-0.236	-1.051	0.201	-1.700	-0.640	-0.718	0.299	0.295	-0.118	0.877
	45	quercetin-3-glucoside	-0.086	0.810	-0.179	-0.116	-0.183	-1.098	-0.538	-0.341	0.140	-1.772	-0.345	1.747
	46	quercitrin	0.625	-0.723	-0.186	0.037	0.220	0.088	0.825	0.994	-0.016	0.327	-0.172	-0.019
	47	rutin	0.170	-0.566	-0.150	-0.105	-0.251	0.483	0.571	0.951	0.035	0.316	-0.241	-0.378
	48	myricetin	-0.547	-1.911	-0.208	-0.402	-0.148	-0.303	0.722	0.280	0.083	0.051	-0.236	-0.235
	49	myricitrin	-0.294	-0.955	-0.051	-0.233	-0.145	0.157	0.758	0.404	0.187	0.336	-0.340	-0.449
isoflavones	50	daidzein	0.655	0.721	1.259	1.162	1.172	1.665	1.666	1.531	1.311	1.519	1.693	2.279
	51	daidzin	0.476	-1.194	0.018	-0.077	-0.384	0.453	0.529	0.828	0.065	0.379	-0.192	-0.140
	52	formononetin	1.108	1.380	1.818	1.505	1.859	1.187	1.931	2.196	2.073	1.778	2.005	1.901
	53	3',4',7-(OH)3-isoflavone	-0.172	0.426	0.475	0.513	-0.693	-1.154	-0.120	1.416	0.108	0.336	0.764	3.390
	54	genistein	1.117	1.290	1.125	1.069	0.959	0.619	1.542	1.694	1.217	0.644	1.858	2.551
	55	genistin	-0.538	-0.978	-0.312	0.108	-0.160	0.478	0.228	0.840	0.191	0.217	-0.206	0.039
	56	prunetin	0.486	0.584	1.092	0.244	-0.435	-1.315	0.456	0.435	1.606	-0.176	2.618	3.395
	57	biochanin A	1.016	1.840	1.518	1.660	1.710	1.748	1.762	2.104	1.741	1.404	1.789	2.420
	58	puerarin	-1.242	-0.387	-0.099	0.014	0.135	0.371	0.802	0.881	0.249	0.238	-0.355	0.037
anthocyan (id)ins	59	pelargonin	-0.561	-0.906	-0.017	-0.165	0.481	0.171	0.390	0.309	0.212	-0.083	0.081	0.548
	60	cyanidin	-1.189	-0.013	-0.233	-0.239	-0.133	-0.660	-0.360	-0.751	-0.040	-0.234	0.065	0.279
	61	keracyanin	0.765	0.578	-0.086	-0.163	-0.171	0.373	0.371	0.418	0.018	0.201	-0.273	-0.329
	62	cyanin	-1.360	0.991	-0.074	-0.225	-0.196	0.316	0.049	0.241	0.185	0.265	-0.476	-0.401
	63	delphinidin	-0.280	-0.135	-0.109	-0.199	-0.006	-1.150	0.218	0.341	0.056	-0.125	-0.091	0.198
	64	oenin	0.184	0.220	-0.099	-0.165	-0.190	-0.815	-0.017	0.139	0.119	-0.021	-0.232	0.218

Fig. 3 Responses of neuroinflammation-related signaling pathways to treatments of BV-2 microglia reporter cells with flavonoids at 10 μM and 50 μM concentrations. Heatmap of the reporter activation expressed as $\log_2$(TF induction fold). See extended Supplementary Table S8 for cell viabilities and SDs

improve viability of Mn(II)-treated microglia. Exceptions are isoflavones as a group, cytotoxic α-naphthoflavone (#15) and flavonol (#36), as well as galangin (#38) and wogonin (#30). Interestingly, isoflavones could increase the viability of IFNγ-treated microglia, while 3,7,8,4′-tetrahydroxyflavone (#41) was the most effective in rescuing the microglia from Mn(II) cytotoxicity. Flavan-3-ols (catechins), flavones, and flavonols attenuated Mn(II)-induced STAT1 activation in microglia, with α-naphthoflavone and flavonol acting as the most potent inhibitors. Other phenolics, including epicatechin gallate (#3), EGCG (#6), 3′,4′-dihydroxyflavone (#17), and myricetin (#48), could counteract the pro-inflammatory activity of manganese (II) in BV-2 microglia, as well. On the other hand, several flavonoids co-operated with Mn(II) in stimulation of the STAT1; the most active were hesperetin (#10), flavone (#14), daidzein (#50), and formononetin

		Base treatment →	None	100 µM Mn	200 µM Mn	IFNγ	None	100 µM Mn	200 µM Mn	IFNγ
		50 µM flavonoids	relative STAT1 activation fold				relative viability			
flavanols	1	catechin	0.352	-0.260	-0.711	-0.110	0.070	0.264	1.009	0.494
	2	epicatechin	0.143	-0.415	-1.017	-0.170	0.154	0.471	1.268	0.541
	3	ECG	-0.026	-1.184	-3.552	-0.573	0.259	0.379	1.239	0.288
	4	GC	-0.138	-0.267	-0.497	-0.076	0.180	0.426	1.318	0.440
	5	EGC	-0.077	-0.340	-0.692	-0.183	0.289	0.291	1.076	0.400
	6	EGCG	0.383	-1.108	-3.572	-0.512	0.209	0.017	0.871	0.353
flavanones	7	naringenin	0.778	0.767	0.450	0.863	0.019	-0.162	0.637	0.134
	8	naringin	-0.198	0.422	0.311	-0.164	0.088	0.178	0.608	0.489
	9	eriodictyol	-1.793	-0.966	-1.820	-0.288	-0.154	0.297	0.709	0.215
	10	hesperetin	0.856	1.588	1.821	1.284	0.095	0.417	0.784	0.435
	11	hesperidin	0.434	-0.294	-0.264	-0.285	-0.005	0.261	0.761	0.320
	12	taxifolin	0.077	-0.604	-0.637	-0.257	0.065	0.340	0.759	0.513
	13	silybin=silibinin	-0.242	0.185	0.425	-0.106	0.057	0.207	0.627	0.444
flavones	14	flavone	0.544	1.140	1.270	1.688	-0.149	0.003	0.493	0.020
	15	α-naphthoflavone	-2.254	-2.856	-6.487	-0.396	-1.743	-0.845	-0.189	-1.736
	16	7-OMe-flavone	1.356	0.074	0.836	1.969	-0.329	0.277	0.803	-0.051
	17	3',4'-(OH)2-flavone	-1.643	-3.756	-4.860	0.628	-0.254	0.657	1.239	-0.301
	18	4',5'-(OH)2-flavone	-0.904	-1.548	-1.353	1.690	-0.215	0.434	0.861	-0.152
	19	4',7-(OMe)2-flavone	0.031	-0.159	0.287	0.549	-0.631	-0.140	0.333	-0.845
	20	5,6-(OH)2-flavone	-2.607	-0.822	-1.012	1.185	-0.402	0.063	0.649	-0.251
	21	chrysin	1.018	0.009	0.231	1.854	0.010	0.068	0.349	-0.004
	22	7,8-(OH)2-flavone	-1.138	-2.878	-2.075	0.250	-0.082	-0.013	0.390	-0.525
	23	2',3',6-(OH)3-flavone	-0.233	-0.789	-1.132	0.380	-0.003	0.353	0.746	-0.136
	24	3',7,8-(OH)3-flavone	-1.448	-1.045	-1.017	-0.315	-0.045	0.380	0.825	0.163
	25	apigenin	-0.471	-3.259	-2.214	1.127	-0.311	0.142	0.741	0.011
	26	acacetin	0.258	-1.733	-1.134	1.259	-0.247	0.072	0.565	0.031
	27	4',7,8-(OH)3-flavone	-0.052	-0.397	-0.316	-0.104	0.001	0.464	0.774	0.251
	28	baicalein	-0.303	-0.456	-0.011	0.358	0.020	0.413	0.836	0.301
	29	baicalin	0.354	-0.079	-1.072	0.582	0.063	0.151	0.568	0.098
	30	wogonin	-0.191	-0.035	0.403	0.821	-0.348	-0.319	-0.383	-0.122
	31	luteolin	-1.607	-0.811	-0.815	0.763	-0.447	0.119	0.461	-0.086
	32	diosmin	-0.251	-0.322	-0.221	-0.363	0.247	0.411	0.662	0.102
	33	neodiosmin	0.304	0.066	0.161	-0.058	0.094	0.271	0.666	0.093
	34	vitexin	0.336	0.140	0.734	0.071	0.129	0.570	0.872	0.153
	35	tangeretin	-0.155	-0.163	0.477	0.643	-0.068	0.138	0.715	-0.102
flavonols	36	flavonol	-2.716	-5.918	-5.403	-1.124	-0.752	-1.679	-0.536	-1.160
	37	4'-OMe-flavonol	1.003	0.078	-0.499	0.614	0.007	-0.041	0.100	-0.007
	38	galangin	0.474	0.491	-0.357	1.247	-0.039	-0.479	-0.219	-0.341
	39	fisetin	-1.863	-0.328	-1.600	0.093	-0.102	0.025	0.398	0.187
	40	kaempferol	0.618	-0.035	-0.767	1.163	-0.055	0.069	0.477	0.237
	41	4',7,8-(OH)3-flavonol	-2.177	-1.012	-0.849	-0.935	0.166	1.351	1.826	1.118
	42	morin	0.407	-0.129	0.323	0.260	0.039	0.623	0.856	0.306
	43	quercetin	-0.944	-0.383	-1.072	-0.243	-0.060	0.305	0.553	0.190
	44	rhamnetin	-1.700	-0.491	-1.098	-0.228	0.325	-0.010	0.381	0.100
	45	quercetin-3-glucoside	-1.098	-0.599	-1.707	-0.208	-0.494	0.124	0.456	-0.111
	46	quercitrin	0.088	-0.022	-0.215	-0.027	0.003	0.075	0.372	0.194
	47	rutin	0.483	0.103	-0.266	-0.139	0.108	0.529	0.640	0.372
	48	myricetin	-0.303	-0.372	-3.851	-0.417	0.176	0.090	0.249	0.234
	49	myricitrin	0.157	0.090	0.049	0.095	0.159	0.102	0.326	0.274
isoflavones	50	daidzein	1.665	1.669	0.759	1.995	0.160	-0.022	0.036	0.262
	51	daidzin	0.453	0.448	0.444	0.147	0.095	-0.381	-0.280	0.071
	52	formononetin	1.187	2.027	2.563	1.762	-0.003	0.298	0.000	0.820
	53	3',4',7-(OH)3-isoflavone	-1.154	-1.183	-1.597	0.647	-0.147	0.309	-0.189	0.494
	54	genistein	0.619	0.138	0.471	1.572	-0.235	-0.097	-0.417	0.725
	55	genistin	0.478	-0.010	0.562	0.127	0.035	0.105	-0.367	0.773
	56	prunetin	-1.315	-1.754	-1.506	0.446	-0.658	-0.189	-0.102	0.028
	57	biochanin A	1.748	0.135	1.003	1.754	-0.066	-0.581	-0.691	0.453
	58	puerarin	0.371	-0.070	0.176	-0.115	-0.017	0.205	0.179	0.050
anthocyan (id)ins	59	pelargonin	0.171	0.273	0.082	-0.167	-0.004	0.174	0.165	0.085
	60	cyanidin	-0.660	-0.057	0.125	-0.022	-0.100	0.192	0.121	0.054
	61	keracyanin	0.373	0.129	0.139	-0.030	0.021	0.225	0.238	0.045
	62	cyanin	0.316	0.280	0.220	-0.135	0.184	0.121	0.243	0.031
	63	delphinidin	-1.150	-0.357	0.008	-0.029	0.293	0.138	0.267	-0.044
	64	oenin	-0.815	-0.348	0.019	0.169	0.220	0.151	0.120	-0.278

Fig. 4 Responses of neuroinflammation-related signaling pathways to treatments of BV-2 microglia reporter cells with combinations of 50 µM flavonoids and manganese(II) at 100 µM or 200 µM, or 50 µM flavonoids and interferon-γ at 1 ng/mL for 12 h. Heatmap of the reporter activation expressed as $\log_2$(relative TF induction fold) and relative viability expressed as $\log_2$(relative GFP expression fold). The relative TF induction and GFP expression folds in columns are calculated as the luciferase activity or GFP fluorescence in the combination-treated cells divided by the luciferase activity/GFP fluorescence in reporter cells subjected to the respective base treatment. See Supplementary Table S9 for the original data source

(#52). Overall, the majority of tested flavonoids were poorly counteracting the pro-inflammatory action of IFNγ and, in fact, about one half in the list did enhance IFNγ-induced transcriptional activation of the STAT1 in BV-2 cells.

One notable pattern seen in Fig. 4 is that the attenuation effects exerted by flavonoids on manganese-treated microglia were more prominent at 200 µM Mn(II) concentrations, as compared to 100 µM Mn(II). To investigate this unexpected effect at other concentrations, we selected three flavonoids, specifically EGCG, apigenin (#25), and myricetin. Unlike EGCG and myricetin, the attenuating effect of apigenin on STAT1 activation decreased in cells treated with 200 µM Mn(II), as compared to those treated with 100 µM Mn(II) (Fig. 4). The combination experiment yielded data presented as contour plots in Fig. 5. Several features can be noted when inspecting Fig. 5: (a) decrease in the STAT1 activation positively correlates with decrease in viability in microglia treated with Mn(II) or apigenin alone; (b) relative to Mn(II)-only treatment, viability of cells treated with Mn(II)/flavonoid combinations generally increased with increasing Mn(II) concentration, even in the case of cytotoxic apigenin; (c) in the Mn(II)/EGCG and Mn(II)/

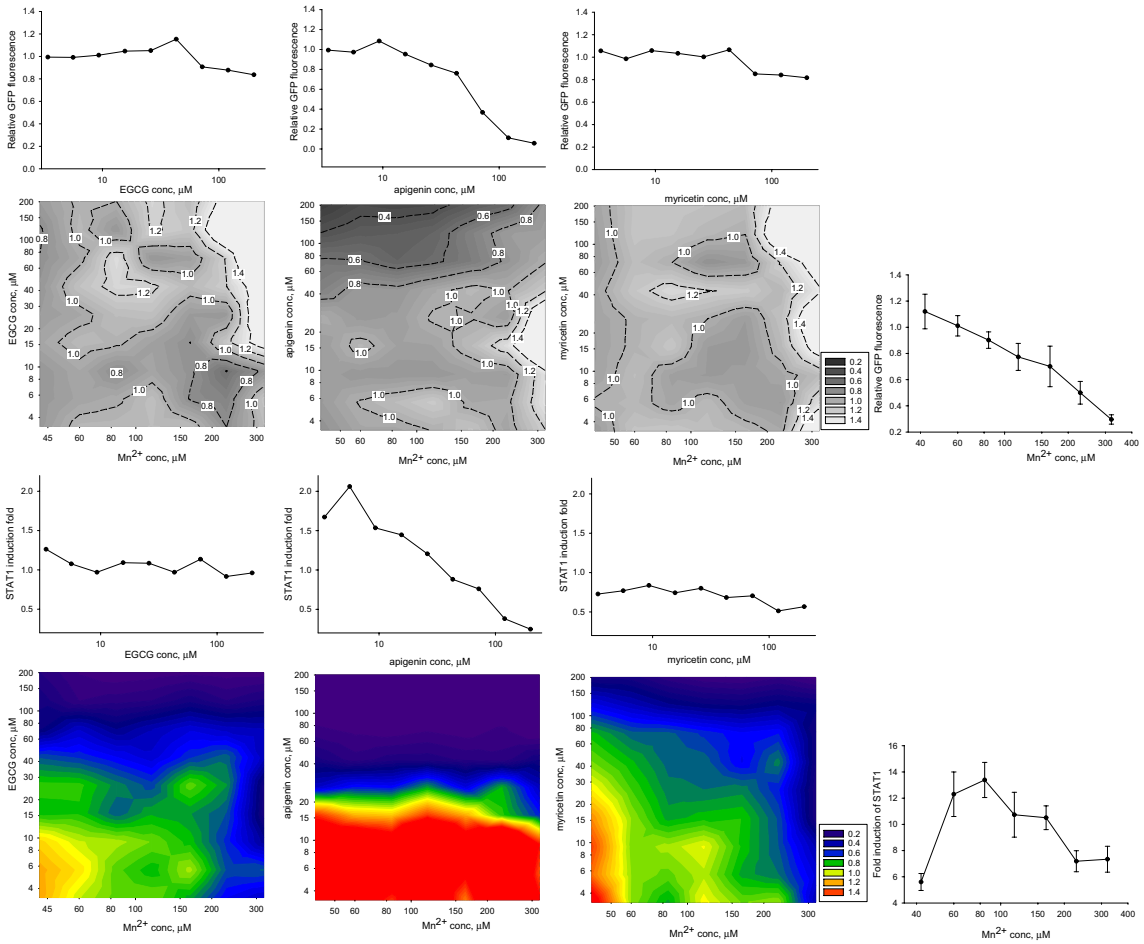

Fig. 5 Viability (two upper rows) and transcriptional activation of homodimer STAT1 (two lower rows) in BV-2 microglia treated with manganese(II) and flavonoids EGCG, apigenin, and myricetin in combinations (contour plots) and alone (satellite line plots) for 12 h. The data points are single measurements or, wherever SD error bars are shown, $n = 3$. For contour plots, relative viability and relative STAT1 activation folds are calculated as in Table 3

myricetin combinations, increase in concentrations of any agent could lead to inhibition of the relative STAT1 activity; (d) apigenin at concentrations below 15 μM could synergize with Mn(II) in the STAT1 activation.

Discussion

An initial goal in this study was to develop a set of neuroinflammation-relevant signaling pathway reporters in a microglia cell line. Our previous experience with integration of the insulated reporter transposons into genomic DNA of several cell types, including an immortalized astrocyte, resulted in generation of multiple reporter cell lines, which demonstrated high consistency of the reporter response over prolonged cell culturing times [29, 31, 35]. The BV-2 microglia, however, has distinguished itself from other cell types by relatively low stability of the reporter activity, in a sense that continuous culturing of these cells without selecting antibiotic puromycin would often lead to decreased GFP and luciferase expression. Nevertheless, careful control of the reporter activity when expanding the cell numbers makes the BV-2 microglia reporters suitable for medium- to high-scale screening studies, as demonstrated in this work.

Our finding that manganese(II) can act as a strong inducer of the interferon-dependent signaling pathways in microglia is novel, and it concurs with the well-documented pro-inflammatory activities of this metal in CNS [15]. The molecular mechanisms of the manganese-induced neuroinflammation were typically explained by the cytotoxicity of this metal [36, 37]. Consequently, the main focus in such studies was on the activities and products of the stress-sensing transcription factors, such as NF-κB, AP-1, and YY1 [15, 18, 38–41]. In one study [22], a gene expression profile in Mn-treated astrocytes showed similarity with that targeted by interferon-γ, which prompted the authors to suggest that

manganese could activate the interferon signaling pathway, even though no increase in the interferon transcription has been detected.

A few in vivo and in vitro studies with peripheral macrophages and other types of immune cells have recognized Mn(II) as an activator of the immune function through induction of type I interferon [42–44]. A proposed mechanism of manganese-stimulated production of type I interferons includes Mn(II) involvement in the cGAS-STING pathway and thus suggests a particular physiological function for manganese in innate anti-viral defense [43]. Taking into account our observations of the lag induction time (Fig. 2) and similarity in activation folds of both homodimer STAT1 and heterodimer STAT1/STAT2 by manganese(II) and IFNα (Fig. 1, Table 2), it would be tempting to ascribe such a role for Mn(II) in microglia, as well. However, a number of other observations obtained in this work cannot be explained based on current models of the manganese-induced macrophage activation. For instance, transcription of type I interferons downstream the cGAS-STING pathway is thought to proceed via the activation of NF-κB [43]. Conversely, in our experiments, the NF-κB activation has lagged well behind the STAT1 and STAT1/STAT2 activation profiles by Mn (Fig. 2). Activation of other transcription factors downstream of the cGAS-STING pathway, such as the interferon regulatory factor IRF3 and STAT6 [45], could be involved in type I interferon expression, as well. Yet, release of IFN-α/β by Mn-stimulated macrophages occurred after about 20-24 hours and reached its maximum at 48-72 hours post treatment [43, 46], while in our experiments, the maximal transcriptional responses of both the homodimer STAT1 and the heterodimer STAT1/2 occurred after only 12 h post-treatment with Mn. Finally, in all aforementioned literature experiments, manganese(II) acted rather as a potentiator than a primary inducer of the interferon production, by co-stimulating macrophages in combinations with viral RNA or DNA, in accord with the cGAS-STING pathway model.

Activation of two other transcription factors, NF-κB and STAT3, by manganese (II) in BV-2 microglia is well in accord with previous reports [19, 39]. The inhibitory effect of this metal on transcriptional activation of the MTF-1 could be related to a competition between Mn^{2+} and Zn^{2+} for their common metal transporters, such as ZIP8, ZIP14, and DMT-1 [47]. On the other hand, the inhibitory effect of Mn(II) on the MAPK/JNK/AP-1 pathway observed by us in BV-2 microglia is in a contrast with data reported by Chen et al. [38].

In order to demonstrate the applicability of the BV-2 microglia-based reporters for large-scale screening studies, we tested responses of the six transcription factors to a set of 64 flavonoids in BV-2 microglia. Since this set was used in our previous study to characterize neuroinflammation-related transcriptional responses to flavonoids in DI TNC1 astrocytes [29], it was possible to compare such responses between these two cell lines. As follows from Fig. 6, there is a consistent positive correlation between transcriptional responses to both 10 μM and 50 μM flavonoids in the microglia and astrocyte reporter lines. Indeed, tested representatives of three structural classes of flavonoids, namely flavanols (##1–6), flavonols (##36–49), and anthocyan(id)ins (##59–64), acted preferentially as inhibitors across multiple signaling pathways, both in BV2 microglia (Fig. 3) and DI TNC1 astrocytes [29]. In both types of cells, isoflavones (##50–58) and a subset of flavones (##14–26) consistently stimulated the transcriptional responses over the basal levels, with several polyphenols, such as flavone, 7-OMe-flavone (#16), 4′,7-$(OMe)_2$-flavone (#19), chrysin, acacetin, daidzein, formononetin, genistein, and biochanin A, acting as the pan-inducers at both 10 μM and 50 μM concentrations. Notably, while in DI TNC1 astrocytes the STAT3 was the most sensitive TF to the inhibition by flavonoids as a whole group [29], in BV2 microglia it was the STAT1 whose activity was suppressed by the largest number of flavonoids at 50 μM (Fig. 3).

In this study, we also demonstrated the utility of the microglia-based TF activation reporters in search for potential antidotes to neurotoxic and neuroinflammatory agents, exemplified in screening of manganese(II)—flavonoid combinations with the STAT1 reporters. Our data (Figure 4) suggest that, even though Mn(II) was presented to the cells in two- to fourfold excess over flavonoids, some polyphenols, such as ECG (#3), EGCG (#6), 3',4'-$(OH)_2$-flavone (#17), or myricetin (#48), could completely negate the cellular responses to the metal in BV2 microglia. There was a direct correlation between effects of flavonoids on the STAT1 activation in presence and in absence of Mn(II) (Fig. 7). No such correlation was found when the effects of flavonoids on the Nrf2 activation were compared with the effects of the combinations on the STAT1 activity. In addition, the interaction patterns for the Mn(II)/flavonoid and the IFNγ/flavonoid combinations were different (Fig. 4). These observations suggest inconsequential roles for metal chelation and antioxidant potential of flavonoids in their STAT1-affecting interactions with manganese (II) in BV-2 microglia.

To the best of our knowledge, this study and our previous report [29] are the first works attempting to assess an array of flavonoids in in vitro models of neuroinflammation. How our data compare to other studies on the neuroprotective potential of flavonoids? In one previous study [48], baicalin at 50 μM modestly decreased the STAT3 phosphorylation (1.2-fold) in amyloid-β treated BV-2 microglia. In our hands, 50 μM baicalin was a weak activator of the all six TFs (Fig. 3), but inhibited the 200 μM Mn(II)-induced STAT1 activation by twofold, along with improved viability of the Mn-treated cells (Fig. 4). Myricetin at 50 μM counteracted hypoxia-induced activation of BV-2 microglia, presumably

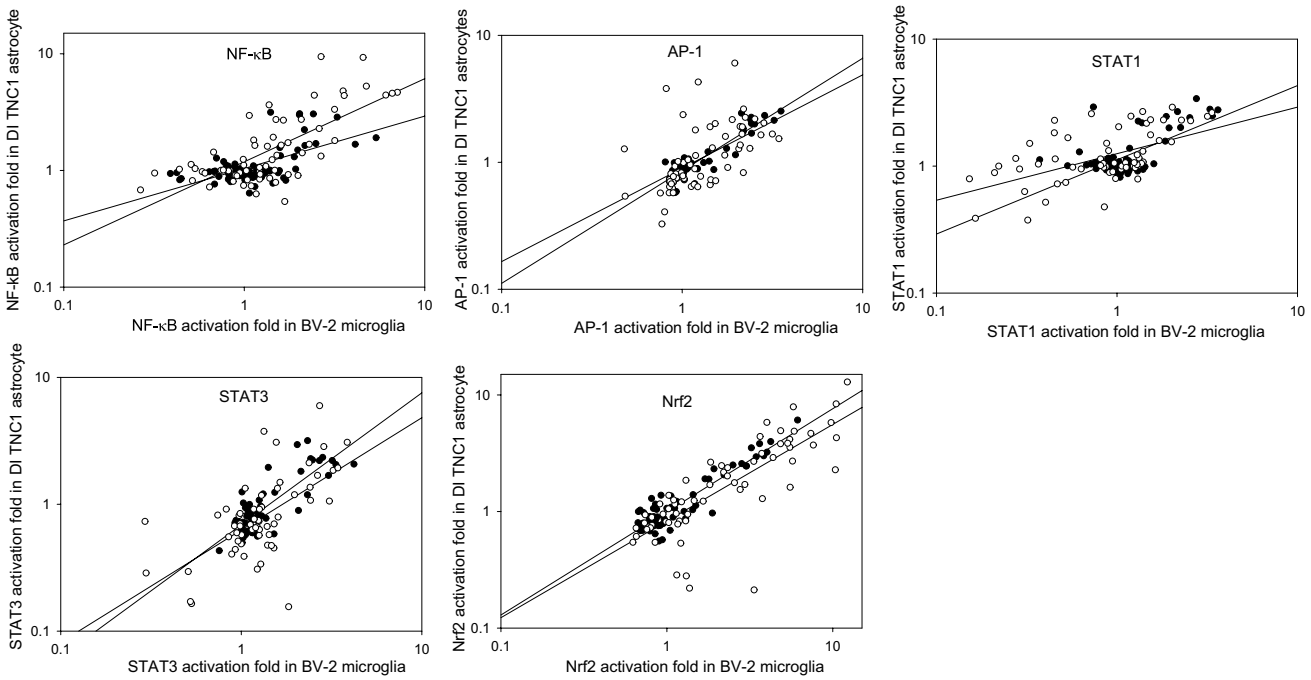

Fig. 6 Correlations between TF responses to 64 flavonoids in BV-2 microglia (this paper) and DI TNC1 astrocytes (reference [29]). Closed and open circles correspond to 10 μM and 50 μM flavonoids, respectively. Each chart contains linear regression plots for both flavonoid concentrations

by inhibiting the STAT1 phosphorylation [49]. In our experiments, 50 μM myricetin showed a weak, 1.2-fold, suppression of the basal STAT1 activation level, but a significant, 14-fold, inhibition of the 200 μM Mn(II)-induced STAT1 activation. Eriodictyol at 50 μM acted as an inducer of the Nrf2 in both BV-2 microglia and in brains of eriodictyol-fed

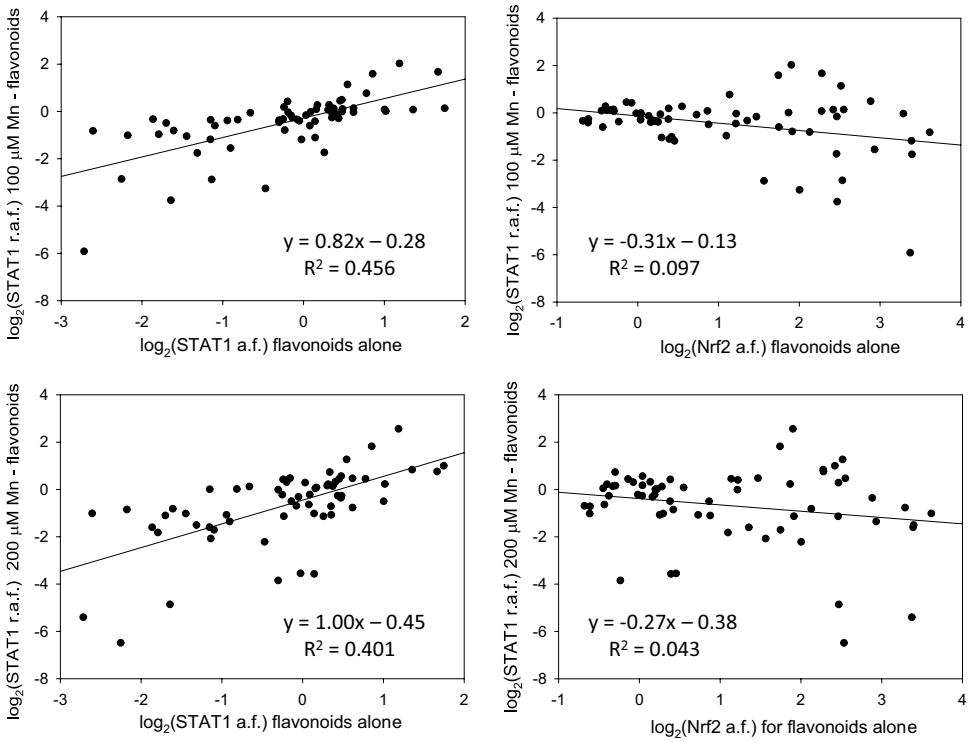

Fig. 7 Correlations between the STAT1 responses to manganese/flavonoids combinations and the STAT1 or Nrf2 responses to flavonoids alone in BV-2 microglia. Sixty four flavonoids were presented to cells at 50 μM in all experiments, Mn(II) - at 100 μM (the upper row) or at 200 μM (the lower row). The activation folds (a.f.) are luciferase activities in flavonoid-only treated cells normalized for the untreated reporter; the relative activation folds (r.a.f.) are luciferase activities in Mn(II)/flavonoid-treated cells normalized for the Mn(II)-only treated reporter

mice [50]. As shown in Figure 3, this flavonoid (#9) at 50 µM activated the Nrf2 as well but acted as a weak inhibitor of the Nrf2 at 10 µM. These examples underscore an advantage of using stable reporters of transcriptional activation for rapid and effective generation of massive data on the cytoprotective potential of multiple flavonoids, as compared to the traditional one-compound-per-study approach. Furthermore, the later approach usually deals with one or limited number of flavonoid concentrations, which, for this class of reactive, multifunctional compounds, may create a problem of bias, due to a well-documented phenomenon of biphasic cellular responses to flavonoids [29, 51]. Therefore, profiling multiple flavonoids, or other sets of biologically interesting agents, by structure and dose, should provide for a systematic landscape of cell-signaling pathways for use in toxicology, pharmacology or nutrition areas. The insulated TF activation reporter transposon platform seems to be an appropriate tool up for the task.

Conclusions

This study demonstrated the utility of insulated transcriptional activity reporter transposon for screening neurotoxic, neuroinflammatory, or neuroprotective agents in microglia. Screening of 12 metals in six reporters of the neuroinflammation-related signaling pathways exposed manganese (II) as a strong inducer of two transcription factors, homodimer STAT1 and heterodimer STAT1/STAT2 in microglia. Screening of an array of 64 flavonoids by this reporter set allowed mapping potentially pro- and anti-inflammatory effects of these agents at two fixed concentrations. Screening combinations of manganese(II) with the flavonoid array revealed potential inhibitors of the cytotoxic and pro-inflammatory activities of Mn(II) in microglia. Results of this in vitro study may inform future laboratory and clinical studies aiming at manganese neurotoxicology, as well as neuroprotective effects of dietary flavonoids.

Supplementary Information The online version contains supplementary material available at https://doi.org/10.1007/s12035-023-03369-w.

Author Contributions VVM: conceptualization, methodology, data collection and analysis, manuscript drafting. JKW: methodology. GYS: conceptualization, resources. ZG: conceptualization, resources. TPM: conceptualization, project administration, and funding acquisition. All authors read and approved the final manuscript.

Funding This research was funded, in part, by the University of Missouri Experiment Station Chemical Laboratories and by the USDA National Institute of Food and Agriculture, Hatch project 1023929.

Data Availability Supporting data are included in the Supplementary Information. All other data are available from the corresponding author upon reasonable request.

Declarations

Ethics Approval Not applicable.

Consent to Participate Not applicable.

Consent for Publication Not applicable.

Competing Interests The authors declare no competing interests.

References

1. Chin-Chan M, Navarro-Yepes J, Quintanilla-Vega B (2015) Environmental pollutants as risk factors for neurodegenerative disorders: Alzheimer and Parkinson diseases. Front Cell Neurosci 9:124. https://doi.org/10.3389/fncel.2015.00124
2. Chen P, Miah MR, Aschner M (2016) Metals and neurodegeneration. F1000Research 5:366. https://doi.org/10.12688/f1000research.7431.1
3. Cotzias GC, Papavasiliou PS, Ginos J, Steck A, Düby S (1971) Metabolic modification of Parkinson's disease and of chronic manganese poisoning. Annu Rev Med 22:305–326. https://doi.org/10.1146/annurev.me.22.020171.001513
4. Dobson AW, Erikson KM, Aschner M (2004) Manganese neurotoxicity. Ann N Y Acad Sci 1012:115–128. https://doi.org/10.1196/annals.1306.009
5. Chtourou Y, Fetoui H, Garoui EM, Boudawara T, Zeghal N (2012) Improvement of cerebellum redox states and cholinergic functions contribute to the beneficial effects of silymarin against manganese-induced neurotoxicity. Neurochem Res 37:469–479. https://doi.org/10.1007/s11064-011-0632-x
6. Lang J, Gao L, Wu J, Meng J, Gao X, Ma H, Yan D (2022) Resveratrol attenuated manganese-induced learning and memory Impairments in mice through PGC-1alpha-mediated autophagy and microglial M1/M2 polarization. Neurochem Res 47:3414–3427. https://doi.org/10.1007/s11064-022-03695-w
7. Ali MF, Taha M (2019) Pathological and hematological studies on the effect of curcumin on manganese chloride-induced neurotoxicity in rats. Compar Clin Pathol 28:69–82. https://doi.org/10.1007/s00580-018-02888-6
8. Bahar E, Kim J-Y, Yoon H (2017) Quercetin attenuates manganese-induced neuroinflammation by alleviating oxidative stress through regulation of apoptosis, iNOS/NF-κB and HO-1/Nrf2 pathways. Int J Mol Sci 18:1989. https://doi.org/10.3390/ijms18091989
9. Hernandez EH, Discalzi G, Valentini C, Venturi F, Chiò A, Carmellino C, Rossi L, Sacchetti A, Pira E (2006) Follow-up of patients affected by manganese-induced Parkinsonism after treatment with $CaNa_2EDTA$. NeuroToxicol 27:333–339. https://doi.org/10.1016/j.neuro.2005.09.003

10. Li S-J, Qin W-X, Peng D-J, Yuan Z-X, He S-N, Luo Y-N, Aschner M, Jiang Y-M, Liang D-Y, Xie B-Y et al (2018) Sodium P-aminosalicylic acid inhibits sub-chronic manganese-induced neuroinflammation in rats by modulating MAPK and COX-2. NeuroToxicol 64:219–229. https://doi.org/10.1016/j.neuro.2017.06.012
11. Ky SQ, Deng HS, Xie PY, Hu W (1992) A report of two cases of chronic serious manganese poisoning treated with sodium para-aminosalicylic acid. Br J Ind Med 49:66–69. https://doi.org/10.1136/oem.49.1.66
12. Akingbade GT, Ijomone OM, Imam A, Aschner M, Ajao MS (2022) D-Ribose-Cysteine attenuates manganese-induced cognitive and motor deficit, oxidative damage, and reactive microglia activation. Environ Toxicol Pharmacol 93:103872. https://doi.org/10.1016/j.etap.2022.103872
13. Kierdorf K, Prinz M (2017) Microglia in steady state. J Clin Invest 127:3201–3209. https://doi.org/10.1172/jci90602
14. Kwon HS, Koh S-H (2020) Neuroinflammation in neurodegenerative disorders: the roles of microglia and astrocytes. Transl Neurodegener 9:42
15. Tjalkens RB, Popichak KA, Kirkley KA (2017) Inflammatory activation of microglia and astrocytes in manganese neurotoxicity. Adv Neurobiol 18:159–181
16. Lee E, Karki P, Johnson J Jr, Hong P, Aschner M (2017) Manganese control of glutamate transporters' gene expression. Adv Neurobiol 16:1–12
17. Harischandra DS, Ghaisas S, Zenitsky G, Jin H, Kanthasamy A, Anantharam V, Kanthasamy AG (2019) Manganese-induced neurotoxicity: new insights into the triad of protein misfolding, mitochondrial impairment, and neuroinflammation. Front Neurosci 13:654
18. Hammond SL, Bantle CM, Popichak KA, Wright KA, Thompson D, Forero C, Kirkley KS, Damale PU, Chong EKP, Tjalkens RB (2020) NF-κB signaling in astrocytes modulates brain inflammation and neuronal injury following sequential exposure to manganese and MPTP during development and aging. Toxicol Sci 177:506–520. https://doi.org/10.1093/toxsci/kfaa115
19. Yin L, Dai Q, Jiang P, Zhu L, Dai H, Yao Z, Liu H, Ma X, Qu L, Jiang J (2018) Manganese exposure facilitates microglial JAK2-STAT3 signaling and consequent secretion of TNF-α and IL-1β to promote neuronal death. NeuroToxicol 64:195–203. https://doi.org/10.1016/j.neuro.2017.04.001
20. Filipov NM, Seegal RF, Lawrence DA (2005) Manganese potentiates *in vitro* production of proinflammatory cytokines and nitric oxide by microglia through a nuclear factor kappa B-dependent mechanism. Toxicol Sci 84:139–148. https://doi.org/10.1093/toxsci/kfi055
21. Liu X, Yao C, Tang Y, Liu X, Duan C, Wang C, Han F, Xiang Y, Wu L, Li Y et al (2022) Role of p53 methylation in manganese-induced cyclooxygenase-2 expression in BV2 microglial cells. Ecotoxicol Environ Saf 241:113824. https://doi.org/10.1016/j.ecoenv.2022.113824
22. Sengupta A, Mense SM, Lan C, Zhou M, Mauro RE, Kellerman L, Bentsman G, Volsky DJ, Louis ED, Graziano JH et al (2007) Gene expression profiling of human primary astrocytes exposed to manganese chloride indicates selective effects on several functions of the cells. NeuroToxicol 28:478–489. https://doi.org/10.1016/j.neuro.2006.10.005
23. O'Shea JJ, Holland SM, Staudt LM (2013) JAKs and STATs in immunity, immunodeficiency, and cancer. N Engl J Med 368:161–170. https://doi.org/10.1056/NEJMra1202117
24. Au-Yeung N, Mandhana R, Horvath Curt M (2013) Transcriptional regulation by STAT1 and STAT2 in the interferon JAK-STAT pathway. Jak-Stat 2:e23931
25. Rauch I, Müller M, Decker T (2013) The regulation of inflammation by interferons and their STATs. Jak-Stat 2:e23820. https://doi.org/10.4161/jkst.23820
26. Hu X, Ivashkiv LB (2009) Cross-regulation of signaling pathways by interferon-γ: implications for immune responses and autoimmune diseases. Immunity 31:539–550. https://doi.org/10.1016/j.immuni.2009.09.002
27. Holtman IR, Skola D, Glass CK (2017) Transcriptional control of microglia phenotypes in health and disease. J Clin Invest 127:3220–3229. https://doi.org/10.1172/jci90604
28. Ivashkiv LB (2018) IFNγ: signalling, epigenetics and roles in immunity, metabolism, disease and cancer immunotherapy. Nat Rev Immunol 18:545–558. https://doi.org/10.1038/s41577-018-0029-z
29. Mossine VV, Waters JK, Gu Z, Sun GY, Mawhinney TP (2022) Bidirectional responses of eight neuroinflammation-related transcriptional factors to 64 flavonoids in astrocytes with transposable insulated signaling pathway reporters. ACS Chem Neurosci 13:613–623. https://doi.org/10.1021/acschemneuro.1c00750
30. Bocchini V, Mazzolla R, Barluzzi R, Blasi E, Sick P, Kettenmann H (1992) An immortalized cell line expresses properties of activated microglial cells. J Neurosci Res 31:616–621. https://doi.org/10.1002/jnr.490310405
31. Mossine VV, Waters JK, Hannink M, Mawhinney TP (2013) *piggyBac* Transposon plus insulators overcome epigenetic silencing to provide for stable signaling pathway reporter cell lines. PLoS One 8:e85494
32. Mossine VV, Waters JK, Chance DL, Mawhinney TP (2016) Transient proteotoxicity of bacterial virulence factor pyocyanin in renal tubular epithelial cells induces ER-related vacuolation and can be efficiently modulated by iron chelators. Toxicol Sci 154:403–415
33. Moreno JA, Sullivan KA, Carbone DL, Hanneman WH, Tjalkens RB (2008) Manganese potentiates nuclear factor-κB-dependent expression of nitric oxide synthase 2 in astrocytes by activating soluble guanylate cyclase and extracellular responsive kinase signaling pathways. J Neurosci Res 86:2028–2038. https://doi.org/10.1002/jnr.21640
34. Bowman AB, Aschner M (2014) Considerations on manganese (Mn) treatments for in vitro studies. NeuroToxicol 41:141–142. https://doi.org/10.1016/j.neuro.2014.01.010
35. Mossine VV, Kelley SP, Waters JK, Mawhinney TP (2023) Screening a small hydrazide-hydrazone combinatorial library for targeting the STAT3 in monocyte-macrophages with insulated reporter transposons. Med Chem Res 32:682–693. https://doi.org/10.1007/s00044-023-03028-8
36. Kraft AD, Harry GJ (2011) Features of microglia and neuroinflammation relevant to environmental exposure and neurotoxicity. Int J Environ Res Public Health 8:2980–3018
37. Pajarillo E, Nyarko-Danquah I, Adinew G, Rizor A, Lee E, Aschner M (2021) Neurotoxicity mechanisms of manganese in the central nervous system. Adv Neurotoxicol 5:215–238
38. Chen C-J, Ou Y-C, Lin S-Y, Liao S-L, Chen S-Y, Chen J-H (2006) Manganese modulates pro-inflammatory gene expression in activated glia. Neurochem Int 49:62–71. https://doi.org/10.1016/j.neuint.2005.12.020
39. Moreno JA, Streifel KM, Sullivan KA, Hanneman WH, Tjalkens RB (2011) Manganese-induced NF-κB activation and nitrosative stress is decreased by estrogen in juvenile mice. Toxicol Sci 122:121–133. https://doi.org/10.1093/toxsci/kfr091
40. Kirkley KS, Popichak KA, Afzali MF, Legare ME, Tjalkens RB (2017) Microglia amplify inflammatory activation of astrocytes in manganese neurotoxicity. J Neuroinflamm 14:99/91-99/18. https://doi.org/10.1186/s12974-017-0871-0
41. Rizor A, Pajarillo E, Son D-S, Aschner M, Lee E (2022) Manganese phosphorylates Yin Yang 1 at serine residues to repress EAAT2 in human H4 astrocytes. Toxicol Lett 355:41–46. https://doi.org/10.1016/j.toxlet.2021.11.007
42. Smialowicz RJ, Luebke RW, Rogers RR, Riddle MM, Rowe DG (1985) Manganese chloride enhances natural cell-mediated

immune effector cell function: effects on macrophages. Immunopharmacology 9:1–11. https://doi.org/10.1016/0162-3109(85)90040-2
43. Wang C, Guan Y, Lv M, Zhang R, Guo Z, Wei X, Du X, Yang J, Li T, Wan Y et al (2018) Manganese increases the sensitivity of the cGAS-STING pathway for double-stranded DNA and is required for the host defense against DNA viruses. Immunity 48(675-687):e677. https://doi.org/10.1016/j.immuni.2018.03.017
44. Song Y, Liu Y, Teo HY, Hanafi ZB, Mei Y, Zhu Y, Chua YL, Lv M, Jiang Z, Liu H (2021) Manganese enhances the antitumor function of CD8+ T cells by inducing type I interferon production. Cell Mol Immunol 18:1571–1574. https://doi.org/10.1038/s41423-020-00524-4
45. Motwani M, Pesiridis S, Fitzgerald KA (2019) DNA sensing by the cGAS-STING pathway in health and disease. Nat Rev Genet 20:657–674. https://doi.org/10.1038/s41576-019-0151-1
46. Sui H, Chen Q, Yang J, Srirattanapirom S, Imamichi T (2022) Manganese enhances DNA- or RNA-mediated innate immune response by inducing phosphorylation of TANK-binding kinase 1. iScience 25:105352. https://doi.org/10.1016/j.isci.2022.105352
47. Chen P, Chakraborty S, Mukhopadhyay S, Lee E, Paoliello MMB, Bowman AB, Aschner M (2015) Manganese homeostasis in the nervous system. J Neurochem 134:601–610. https://doi.org/10.1111/jnc.13170
48. Xiong J, Wang C, Chen H, Hu Y, Tian L, Pan J, Geng M (2014) Aβ-induced microglial cell activation is inhibited by baicalin through the JAK2/STAT3 signaling pathway. Int J Neurosci 124:609–620
49. Boriero D, Carcereri de Prati A, Antonini L, Ragno R, Sohji K, Mariotto S, Butturini E (2021) The anti-STAT1 polyphenol myricetin inhibits M1 microglia activation and counteracts neuronal death. FEBS J 288:2347–2359. https://doi.org/10.1111/febs.15577
50. He P, Yan S, Wen X, Zhang S, Liu Z, Liu X, Xiao C (2019) Eriodictyol alleviates lipopolysaccharide-triggered oxidative stress and synaptic dysfunctions in BV-2 microglial cells and mouse brain. J Cell Biochem 120:14756–14770. https://doi.org/10.1002/jcb.28736
51. Chirumbolo S (2010) The role of quercetin, flavonols and flavones in modulating inflammatory cell function. Inflamm Allergy Drug Targets 9:263–285. https://doi.org/10.2174/187152810793358741